Exciton Quenching Close to Polymer−Vacuum Interface of Spin-Coated Films of Poly(*p*-phenylenevinylene) Derivative

Oleksandr V. Mikhnenko,*,†,‡ Fabrizio Cordella,† Alexander B. Sieval,§ Jan C. Hummelen,†,∥ Paul W. M. Blom,†,⊥ and Maria Antonietta Loi*,†

Zernike Institute for Advanced Materials, University of Groningen, Nijenborgh 4, 9747 AG Groningen, The Netherlands, Dutch Polymer Institute, P.O. Box 902, 5600 AX, Eindhoven, The Netherlands, Solenne BV, Zernikepark 6-8, 9747 AN, Groningen, The Netherlands, Stratingh Institute for Chemistry, Nijenborgh 4, 9747 AG Groningen, University of Groningen, The Netherlands, Holst Centre, High Tech Campus 31, 5656 AA, Eindhoven, The Netherlands

Received: February 11, 2009; Revised Manuscript Received: May 14, 2009

Polymer−fullerene bilayer heterostructures are suited to study excitonic processes in conjugated polymers. Excitons are efficiently quenched at the polymer−fullerene interface, whereas the polymer−vacuum interface is often considered as an exciton-reflecting interface. Here, we report about efficient exciton quenching close to the polymer−vacuum interface of spin-coated MDMO-PPV (poly[2-methoxy-5-(2′-ethyl-hexyloxy)-*p*-phenylenevinylene]) films. The quenching efficiency is estimated to be as high as that of the polymer−fullerene interface. This efficient quenching is consistent with enhanced intermolecular interactions close to the polymer−vacuum interface due to the formation of a "skin layer" during the spin-coating procedure. In the skin layer, the polymer density is higher; that is, the intermolecular distances are shorter than in the rest of the film. The effect of exciton quenching at the polymer−vacuum interface should be taken into account when the thickness of the polymer film is on the order of the exciton diffusion length; in particular, in the determination of the exciton diffusion length.

Introduction

Spin-coating or spin-casting is a thin film deposition technique from solution that is conducted by first wetting and then spinning a flat substrate. Depending on the rotation speed, the solution experiences centrifugal forces that, together with the solvent evaporation process, are responsible for the film formation. Spin-coating is a versatile deposition method that is used for various applications; for instance, to deposit photoresists or dielectric layers in microcircuit technology, to fabricate antireflection coatings for optical applications, or magnetic coatings in the data storage industry. Furthermore, spin-coating is used to deposit thin films of conjugated polymers to fabricate solar cells, field effect transistors, light-emitting diodes, etc.

Conjugated polymers show semiconducting properties and can be designed to be soluble in common organic solvents. For low-cost electronic devices, however, spin-coating is not as cost-effective as printing techniques, which are the most promising deposition methods for mass production.[1] Nevertheless, in contrast to other techniques, spin-coating is simple, well understood,[2,3] easy to control, and allows preparation of thin films of precise thicknesses. Therefore, it is an excellent deposition technique to investigate properties of conjugated polymers as well as to optimize devices based on them.

Over the past few decades the morphology of spin-coated polymer films has been studied extensively. It was predicted theoretically[2,3] and shown experimentally[4,5] that close to the polymer-vacuum interface, a "skin layer" is formed, which is characterized by a high density and in-plane ordering of molecular chains (Figure 1). The rest of the film has uniform density, which is shown to be 3 times less than the density of the skin layer in a typical conjugated polymer, such as poly[2-methoxy-5-(2′-ethyl-hexyloxy)-*p*-phenylenevinylene] (MEH-PPV).[5] Because of such a density difference, the rest of the film is sometimes regarded as a "spongy layer".

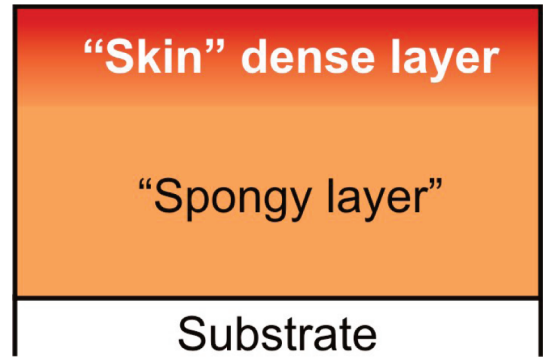

Figure 1. The bilayered structure of a spin-coated polymer film.

The skin layer formation originates from the rapid solvent evaporation at the free surface, which leads to a local increase in the polymer concentration during spinning. This rise in the concentration can be so abrupt that the polymer becomes almost solid close to the surface, which slows down the solvent evaporation rate from the rest of the forming film.[3] Even when the film is fully formed, some of the solvent remains trapped below the skin layer. Usually, such solvent residuals are removed by vacuum baking. At this stage, the polymer viscosity is so high that the long chains cannot fill the space that was previously

* Corresponding authors. E-mails: (O.V.M.) O.Mikhnenko@rug.nl, (M.A.L.) M.A.Loi@rug.nl.
† Zernike Institute for Advanced Materials, University of Groningen.
‡ Dutch Polymer Institute.
§ Solenne BV.
∥ Stratingh Institute for Chemistry, University of Groningen.
⊥ Holst Centre.

10.1021/jp9012637 CCC: $40.75
Published on Web 06/15/2009

filled by the solvent residuals. Thus, a spongy layer is formed below the skin of the film.

The influence of the skin layer on the physical parameters, such as glass transition temperature[6,7] and anisotropy of the refractive index,[8,9] becomes apparent in relatively thin films, when the skin layer is a considerable part of the total film thickness. The relevant thickness range depends on the polymer properties, the solvent evaporation rate, and the spin conditions. In relatively thick films, the spongy layer dominates the total film volume, which results in thickness-independent film properties.

In this contribution, we report about the influence of the skin layer on the measurements of the exciton dynamics in conjugated polymers. In this class of materials, excitons are the primary optical excitations, and they can be considered as bound, localized electron−hole pairs. Once created, they tend to diffuse among conjugated segments by means of energy transfer. The average displacement of an exciton during its lifetime is called the exciton diffusion length. This parameter is very important in the design of organic solar cells because it determines the volume of the conjugated polymer from which excitons can reach the dissociation interface, where they can be separated into free electrons and holes to contribute to photocurrent.[10] The measurement of the exciton diffusion length is therefore important both for the engineering of optoelectronic devices and for the fundamental knowledge about conjugated polymers.

The exciton diffusion length is often extracted from photoluminescence (PL) measurements by varying the thickness of the polymer film, which is deposited on top of an exciton quenching layer.[10−17] When the polymer thickness is decreased to the order of the exciton diffusion length, the PL decay times in such a polymer−quencher heterostructure become shorter than those in the relatively thick films. The exciton diffusion length can then be estimated by modeling the thickness dependence of the PL decay process. The influence of the skin layer at the polymer−vacuum interface is usually neglected in such models, because it is assumed that excitons are reflected by this free interface.

Here, we study the exciton behavior in the skin layer of spin-coated MDMO-PPV (poly[2-methyl-5-(3′,7′-dimethyloctyloxy)-*p*-phenylenevinylene]) films. We chose this soluble derivative of PPV because it has been widely used in solar cell research.[18] For this class of materials, the exciton diffusion length is typically reported in the range of 5−7 nm.[10,11,13−15,19−21] To extract the exciton diffusion length using polymer−quencher heterostructures, the polymer thickness should be varied in the range of 5−50 nm for MDMO-PPV. Absorption spectroscopy reveals that in this thickness range, the skin layer considerably contributes to the total film thickness and, thus, cannot be neglected. We show that the PL decay times of the pristine MDMO-PPV films, spin-coated on quartz substrates, exhibit a thickness dependence similar to that of the polymer−quencher heterostructures. Such thickness dependence is caused by the efficient exciton quenching in the skin layer. The efficiency of this quenching can be estimated by measuring the exciton diffusion length both in the pristine films and in polymer−quencher heterostructures. The values of the exciton diffusion length, which are extracted from both kinds of samples, correspond to each other only if we assume that the exciton quenching in the skin layer is as efficient as the quenching at the polymer−fullerene interface, which is well-known for its high exciton quenching efficiency.[10,22,23]

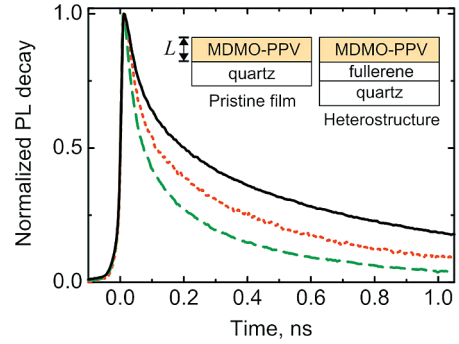

Figure 2. PL decays of pristine MDMO-PPV film (dotted line) and heterostructure (dashed line) of the same polymer thickness, 13 nm. The PL decay of 240-nm-thick reference pristine film is also shown (solid line). The PL decays are normalized to its maximum value. The inset shows the composition of the pristine films and the heterostructures.

Experimental Methods

MDMO-PPV was spin-coated from chlorobenzene on top of clean quartz substrates and insoluble[14] cross-linked fullerene films, poly(F2D), to form the pristine films and heterostructures, respectively (inset to Figure 2). The spin speed of 2000 rpm was kept constant for all the samples, and the polymer thickness variation was ensured by changing the solution concentration. The sample preparation was done under nitrogen atmosphere.

The surfaces of the quartz substrates, of poly(F2D), and of MDMO-PPV were characterized by atomic force microscopy (AFM). The root-mean-square roughness was found to be <1 nm for all the surfaces on an area of 100 μm^2. The thicknesses of organic layers were measured by AFM and nulling-zone ellipsometry. The thickness of poly(F2D) was kept to <30 nm in all the heterostructures.

PL decays, continuous wave (cw) absorption, and PL spectra were measured for every sample. Time-resolved measurements were performed, exciting the samples with 100 fs laser pulses, produced by a Ti−sapphire laser and frequency-doubled at about 400 nm; the PL decays were recorded by a Hamamatsu streak camera. The initial exciton density was estimated to be $\sim 10^{13}-10^{14}$ cm^{-3}, being several orders of magnitude less than needed for exciton−exciton annihilation.[24] The cw PL spectra were measured using a Hamamatsu CCD, and the absorption spectra were obtained with a Perkin-Elmer spectrometer. The samples were kept in a dynamic vacuum of $10^{-6}-10^{-5}$ mbar during the photoluminescence measurements, and no degradation was observed. For the absorption measurements, the samples were sealed in a chamber under nitrogen atmosphere.

For analysis, the decays were spectrally integrated and normalized to the maximum value. It was verified that optical interference and self-absorption effects can be safely ignored in the thickness range studied here.

Results and Discussions

Thickness Dependence of the PL Decay Times. Figure 2 shows the PL decays (i) of a 240-nm-thick polymer film serving as the reference sample (solid line) and (ii) of the heterostructure (dashed line) and the pristine film (dotted line), each of them with a polymer thickness of 13 nm. The PL decay times depend on polymer thickness for both heterostructures and pristine films, being faster for thinner samples. The dependence is monotonic and appears to be strongest in the polymer thickness range between 5 and 50 nm, whereas >200 nm thick films are characterized by a thickness-independent PL decay. As stated

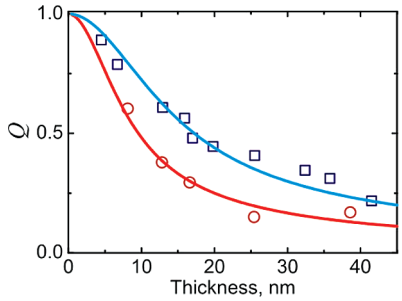

Figure 3. Measured relative quenching efficiency, Q, of the pristine films (circles) and the heterostructures (squares). The curves represent the best fits with eqs 8 and 7, respectively.

above, excitons are efficiently quenched at the polymer−fullerene interface;[10,22,23] the number of excitons that reach the interface is limited by the exciton diffusion length L_D.[23] Consequently, for polymer thicknesses approaching L_D, the relative number of quenched excitons in the heterostructure is increased, leading to shorter PL decay times (Figure 2, dashed line).

The dotted line in Figure 2 shows that the PL decay times of pristine MDMO-PPV films depend on thickness in a manner similar to the heterostructures, being shorter for thinner films. Such thickness dependence can be ascribed to exciton quenching at one or both interfaces of the pristine polymer film. We will show that the skin layer of a spin-coated MDMO-PPV film quenches excitons with an efficiency similar to that of a polymer−fullerene interface.

To quantify the overall exciton quenching in a polymer film, we introduce the relative quenching efficiency $Q(L)$:

$$Q(L) = 1 - \frac{\text{total PL of sample with polymer thickness } L}{\text{total PL of thick reference sample}} \quad (1)$$

where the total PL is the time integral of the PL decay normalized to its maximum value, and the reference sample is a >200 nm thick MDMO-PPV film. The thickness dependencies of the relative quenching efficiency were measured for both pristine films and heterostructures. They are shown in Figure 3 as circles and squares, respectively. In general, the overall quenching in the heterostructures was found to be more efficient than in pristine films. Hence, we can estimate that the quenching efficiency of the polymer−quartz interface is much smaller than that of the polymer−fullerene interface. On the other hand, if the exciton quenching efficiency is small or zero at the polymer−quartz interface, then the excitons should be quenched efficiently close to the polymer−vacuum interface (i.e. in the skin layer) to explain the pronounced thickness dependence $Q(L)$ for the pristine films (Figure 3).

To independently quantify the exciton quenching at polymer−quartz interface and in the skin layer of a MDMO-PPV film, we will assume that the characteristics of the skin layer are essentially the same in the heterostructures and the pristine films.[25,26] In the next section, we will quantify the quenching efficiency by following this hypothesis.

***L_D* Measurements.** The exciton diffusion length in polymer films is often measured using the diffusion-limited quenching at the interface with either fullerenes or fullerene derivatives,[11,12,14,19−21] titania,[13,15] or metals.[16] The dependence of the relative quenching efficiency, Q, on the polymer thickness, L, is recorded experimentally, and it is fitted with a mathematical model based on a diffusion equation. Such a fitting results in a value of L_D typically in the range of 5−7 nm for PPV derivatives.[10,11,13−15,19−21]

Here, we measure the exciton diffusion length to estimate the efficiency of the exciton quenching in the skin layer. For simplicity, we will neglect the finite thickness of the skin layer in the modeling. Then the quenching in this layer can be considered as an interface effect. Later, we will estimate the influence of a finite thickness of the skin layer on our results.

The exciton diffusion length is an intrinsic property of the conjugated polymer and should be the same in the heterostructures and the pristine films. Since in our sample geometry, the effect of interface quenching enters the diffusion model as boundary conditions, we can estimate the efficiencies of such quenching simply by choosing the boundary conditions that lead to the proper value of L_D for both types of samples.

The exciton density, n, is modeled by the following diffusion equation:

$$\partial_t n(x,t) = -n(x,t)/\tau + D\,\partial_{xx} n(x,t) + G(x,t) - S(x)\,n(x,t) \quad (2)$$

where τ denotes the exciton lifetime and D is the exciton diffusion coefficient that is related to the diffusion length by the equation $L_D = (D\tau)^{1/2}$. Due to the sample symmetry, n depends only on one spatial coordinate x, which is the distance from the free interface. Because ultrafast photo excitation has been used, the generation term $G(x, t)$ can be represented as the initial exciton distribution, which is taken to be uniform due to the low absorption coefficient at the excitation wavelength.

The term $S(x)$ in eq 2 denotes the interface quenching; it can be adjusted to mimic different boundary conditions. The polymer−vacuum interfaces of the heterostructures and the pristine films are assumed to be equal, implying common boundary conditions at this interface for both sorts of samples. As we noted in the previous section, the quenching efficiency of the polymer−vacuum interface is expected to be high. In our modeling, we assume it to be 100% efficient:

$$n(0,t) = 0 \quad (3)$$

The polymer−fullerene interface is known to be an efficient exciton quencher, which provides the second boundary condition for the heterostructures with polymer thickness L:

$$n(L,t) = 0 \quad (4)$$

The polymer−quartz interface is expected to be a weak exciton quencher; therefore, here, we assume that its quenching efficiency is negligible:

$$\partial_x n(L,t) = 0 \quad (5)$$

With these boundary conditions, eq 2 can be simplified to Cauchy problems and solved analytically for both types of samples. Then the relative quenching efficiency Q is simply

$$Q(L, L_D) = 1 - \frac{\int_0^L \mathrm{d}x \int_0^\infty n_{\text{quenched sample}}(x,t)\,\mathrm{d}t}{LN_0\tau} \quad (6)$$

where $LN_0\tau$ is the total PL of a quencher free sample. Integration of eq 6 leads to the analytical expressions Q_2 and Q_1 for the heterostructures and the pristine films, respectively:

$$Q_2(L, L_D) = \frac{2L_D}{L} \tanh \frac{L}{2L_D} \quad (7)$$

$$Q_1(L, L_D) = \frac{L_D}{L} \tanh \frac{L}{L_D} \quad (8)$$

Here, the exciton diffusion length, L_D, is the only fitting parameter, and the index near Q denotes the number of quenching interfaces.

The fitting of the experimental data for the heterostructures and the pristine films by eqs 7 and 8 is illustrated in Figure 3. The resulting values of the exciton diffusion length are 4.5 and 5 nm, respectively. These values are similar and were extracted from two different series of samples under the common assumption that the polymer−vacuum interface efficiently quenches excitons. It is important to note that the extracted values of the exciton diffusion length correspond to the one of the spongy layer.

These values would diverge when the boundary condition at the polymer−vacuum interface would be varied to reduce the quenching efficiency. In the limiting case, when the quenching efficiency of the polymer−vacuum interface approaches zero, the extracted exciton diffusion length from the heterostructures would be close to 9 nm, whereas that from the pristine films will virtually approach infinity. Thus, we can conclude that our assumption of efficient exciton quenching at the polymer−vacuum interface is correct because it leads to the similar values of the exciton diffusion length, extracted from either kind of sample.

Skin Layer in Spin-Coated Films. The theoretical prediction[2,3] of a dense skin layer close to the free interface (Figure 1) was followed by the experimental confirmation of a bilayered film structure. On the basis of neutron reflection experiments on spin-coated MEH-PPV films, Webster et al.[5] concluded that such films are composed of two well-defined and uniform layers of different densities. They reported a density ratio as high as 3 between a 24 nm, thin, dense layer and a 136 nm, thick, "spongy" layer. Lu and coauthors[4] discovered the bilayered structure of spin-coated polyacrylamide films by reflection−absorption Fourier transform infrared spectroscopy. The molecules in the part of the layer closest to the substrate were found to be randomly oriented, whereas the skin layer[4] showed spin-coating-induced in-plane chain orientation.[8,27,28] Moreover, the idea of a bilayered structure of spin-coated films is also often used to explain the thickness dependence of the glass transition temperature in conjugated polymers.[6,7] Here, we report spectroscopic evidence of the bilayered structure of a thin polymer film, which confirms the exciton quenching effect in the skin layer.

The absorption spectrum of MDMO-PPV films exhibits a thickness dependence that is equal for heterostructures and pristine films (Figure 4). Figure 5 displays the variation of the energy maximum of the absorption spectrum for films of different thicknesses. The absorption maximum shifts by 0.14 eV toward lower energies, going from >200 nm to ∼15 nm thickness. A further thickness decrease leads to the opposite trend; that is, to a blue shift. This thickness dependence is relatively strong. For comparison, the Stokes shift for the 240 nm thick MDMO-PPV film is 0.34 eV (Figure 5), and the typical

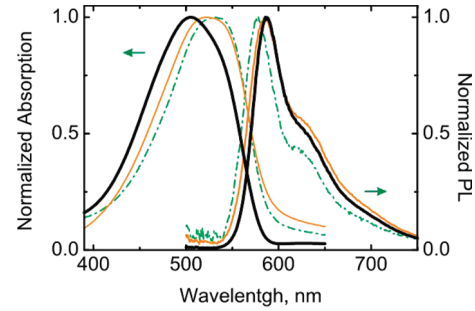

Figure 4. Normalized absorption and normalized photoluminescence spectra of polymer films with thicknesses 240 nm (solid, thick line), 42 nm (solid, thin line) and 7 nm (dashed−dotted line). The spectra are normalized to their maximum values.

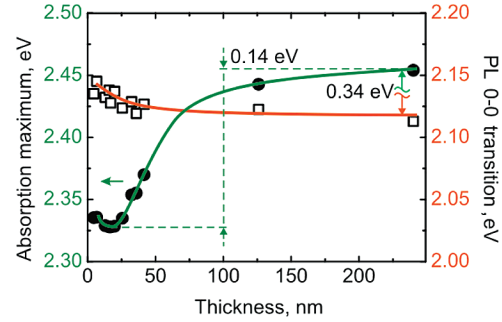

Figure 5. Measured thickness dependencies of the maximum position of the absorption spectrum (circles) and 0−0 PL transition (squares). The curves are shown as guides for eyes.

value for the half-width of the Gaussian excitonic density of states[29] is ∼0.1 eV.

The thickness dependence of the absorption spectrum can be explained in terms of the bilayered structure of spin-coated polymer films. As mentioned previously, the spin-coating procedure induces in-plane chain orientation in the skin layer of the film,[4,8,27,28] whereas the polymer chains adopt random conformations in the spongy layer (Figure 1). Consequently, the skin layer is characterized by polymer chains with longer average conjugation length and by the red-shifted absorption,[30] as compared to the spongy one. In >200 nm thick films, the absorption spectrum is dominated by the spongy layer, whereas in thinner films, the skin layer becomes more valuable, leading to the red shift (Figure 5). For ultrathin films with thicknesses below 15 nm, the influence of the substrate dominates over the spin-coating-induced effects, resulting in the blue shift upon further thickness decrease.

One would expect that the exciton migration process is anisotropic at the interface between the two layers of the spin-coated polymer film. Indeed, due to the different degrees of ordering, a gradient of the conjugation length is formed between such layers. Since the excitons tend to migrate toward longer conjugated segments, one rather would expect a drift directed to the better-ordered skin layer than an isotropic diffusion process. Such a drift depletes the exciton population in the spongy layer and increases it in the skin layer. Since the density of states is considerably shifted toward lower energy in the skin layer, one would expect that any PL from the skin layer would be red-shifted. This would apply to samples in the thickness range of 5−50 nm.

Figure 4 shows the steady-state PL spectra that correspond to the polymer films of thicknesses 7, 42, and 240 nm. Figure 5 summarizes the thickness dependence of the maximum position of the PL 0−0 transition. The dependence is weaker

than that of the absorption spectrum; moreover, we can resolve a monotonic shift to *higher* energy with a thickness decrease in the range of 5−50 nm. It is important to note that we did not find substantial differences in the peak positions of the PL spectra between heterostructures and the corresponding pristine films.

We attribute the absence of the expected red shift of the PL spectrum to the exciton quenching in the skin layer of the spin-coated film. The observed photoluminescence is mostly coming from the spongy layer, which is not influenced by the spin-coating procedure, and thus, its degree of ordering does not depend on the sample thickness. In the thickness range of 5−20 nm, most of the excitons reach a quenching interface; thus, the observed photoluminescence is originated at the early stages of the exciton diffusion. During roughly the first 100 ps after the laser pulse, excitons undergo a thermalization process; that is, a downhill migration toward lower energy sites.[31] The photons emitted during this process are blue-shifted as compared to the emission of thermalized excitons. In sufficiently thin films, excitons get quenched before the completion of thermalization. Therefore, we observe a slight blue shift for films with thicknesses close to the exciton diffusion length (Figure 5).

One of the physical phenomena responsible for the exciton quenching in the skin dense layer can be the interchain coupling that leads to formation of nonradiative dark states. Ruini at al.[32] performed ab initio calculations of PL intensity and real space exciton wave function for both PPV crystal and an isolated chain, showing that in the crystal, the lowest electronic excitation is an optically inactive exciton. They also noted that the PL efficiency would strongly depend on the local polymer density, being lower for more densely packed chains. Nguyen et al.,[33] using scanning near-field optical microscopy, showed experimentally that the PL intensity is weaker from the denser clusters of an inhomogeneous MEH-PPV film. The concept of exciton quenching due to interchain interactions is supported by numerous reports on decrease of the PL quantum yield under application of hydrostatic pressure in various organic materials.[34−36]

Our measurements show that the PL is quenched with high efficiency in the skin layer. Such a high quenching efficiency reflects the high number of excitons that decay nonradiatively close to the polymer−vacuum interface. It is energetically favorable for excitons to migrate into the region of higher density, which is characterized by longer average conjugation length. Since the film density increases when going from the spongy layer to the skin layer, excitons would rather drift into the latter than anisotropically diffuse between the layers. In this way, the exciton concentration increases in the skin dense layer, where the probability of nonradiative decay is high.[32−36] As a result, the number of excitons that decay nonradiatively increases, and finally, the exciton quenching within the skin layer can be approximated as the 100% efficient quenching at the polymer−vacuum interface.

It is important to note that in the bilayered spin-coated film, the conformations of the polymer chains in the vicinity of the free surface are decoupled from the substrate and are fully determined by the spin-coating conditions. The detailed surface analyses of spin-coated poly(3-hexylthiophene) films by ultraviolet photoelectron spectroscopy, Penning ionization electron spectroscopy,[26] and X-ray absorption fine structure spectroscopy[25,26] show that the polymer chain conformation at the surface does not change upon thickness variation, obtained by changing the polymer concentration and keeping the spin speed constant. This supports our assumption that the skin layer is essentially the same for both the heterostructure and the pristine film of corresponding thickness.

Finally, we address the neglect of the skin layer thickness in our modeling of the relative quenching efficiency. Every exciton that passes from the spongy to the dense layer does not diffuse back due to the energy gradient, but subsequently decays nonradiatively due to the effect of enhanced density.[32−36] The interface between the dense and the spongy layers is reported to be relatively sharp.[5] Thus, this interface, not that of the polymer−vacuum, should be considered as the exciton quenching wall in our modeling. Consequently, we should use the thickness of the spongy layer instead of the overall film thickness, L, in the modeling.

Although we had no opportunity to reliably estimate the thicknesses of the skin and spongy layers, the obtained results of the exciton diffusion length still allow us to draw our main conclusion. Suppose the thickness of the skin layer is about 10% of the overall film thickness, L. Then the thickness of the spongy layer is 0.9 L, which should be put into the modeling as a sample thickness. Since the relative quenching efficiencies (eqs 7 and 8) depend on the ratio L/L_D, the resulting values of the exciton diffusion length would be smaller than the obtained ones with a factor of 0.9 for both the heterostructures and the pristine films. This means that neglecting the skin layer thickness affects the *absolute values* of the measured exciton diffusion length, but not the *ratio* between them. Thus, we can still compare those values and conclude that the skin layer efficiently quenches excitons.

Conclusions

We showed that in the skin layer of spin-coated MDMO-PPV film excitons are quenched with high efficiency, comparable to that of a polymer−fullerene interface. One of the physical phenomena responsible for such a quenching is the formation of nonradiative dark states close to the polymer−vacuum interface due to higher polymer density. This effect should be taken into account for films in the thickness range 5−50 nm, in particular when the exciton population is measured or estimated.

Acknowledgment. The work of O. V. Mikhnenko forms part of the research program of the Dutch Polymer Institute (Project no. 518). The authors thank F. v. d. Horst and J. Harkema for the technical support.

References and Notes

(1) Brabec, C. J.; Durrant, J. R. *MRS Bull.* **2008**, *33*, 670.
(2) Lawrence, C. J. *Phys. Fluids* **1988**, *31*, 2786.
(3) Bornside, D. E.; Macosko, C. W.; Scriven, L. E. *J. Appl. Phys.* **1989**, *66*, 5185.
(4) Lu, X.; Cheng, I.; Mi, Y. *Polymer* **2007**, *48*, 682.
(5) Webster, G. R.; Mitchell, W. J.; Burn, P. L.; Thomas, R. K.; Fragneto, G.; Markham, J. P. J.; Samuel, I. D. W. *J. Appl. Phys.* **2002**, *91*, 9066.
(6) Campoy-Quiles, M.; Sims, M.; Etchegoin, P. G.; Bradley, D. D. C. *Macromolecules* **2006**, *39*, 7673.
(7) Forrest, J. A.; Dalnoki-Veress, K.; Stevens, J. R.; Dutcher, J. R. *Phys. Rev. Lett.* **1996**, *77*, 2002.
(8) Campoy-Quiles, M.; Etchegoin, P. G.; Bradley, D. D. C. *Phys. Rev. B* **2005**, *72*, 045209.
(9) Sturm, J.; Tasch, S.; Niko, A.; Leising, G.; Toussaere, E.; Zyss, J.; Kowalczyk, T. C.; Singer, K. D.; Scherf, U.; Huber, J. *Thin Solid Films* **1997**, *298*, 138.
(10) Peumans, P.; Yakimov, A.; Forrest, S. R. *J. Appl. Phys.* **2003**, *93*, 3693.
(11) Halls, J. J. M.; Pichler, K.; Friend, R. H.; Moratti, S. C.; Holmes, A. B. *Appl. Phys. Lett.* **1996**, *68*, 3120.

(12) Haugeneder, A.; Neges, M.; Kallinger, C.; Spirkl, W.; Lemmer, U.; Feldmann, J.; Scherf, U.; Harth, E.; Gügel, A.; Müllen, K. *Phys. Rev. B* **1999**, *59*, 15346.
(13) Kroeze, J. E.; Savenije, T. J.; Vermeulen, M. J. W.; Warman, J. M. *J. Phys. Chem. B* **2003**, *107*, 7696.
(14) Markov, D. E.; Amsterdam, E.; Blom, P. W. M.; Sieval, A. B.; Hummelen, J. C. *J. Phys. Chem. A* **2005**, *109*, 5266.
(15) Scully, S. R.; McGehee, M. D. *J. Appl. Phys.* **2006**, *100*, 034907.
(16) Wu, Y.; Zhou, Y. C.; Wu, H. R.; Zhan, Y. Q.; Zhou, J.; Zhang, S. T.; Zhao, J. M.; Wang, Z. J.; Ding, X. M.; Hou, X. Y. *Appl. Phys. Lett.* **2005**, *87*, 044104.
(17) Zhou, Y. C.; Wu, Y.; Ma, L. L.; Zhou, J.; Ding, X. M.; Hou, X. Y. *J. Appl. Phys.* **2006**, *100*, 023712.
(18) Shaheen, S. E.; Brabec, C. J.; Sariciftci, N. S.; Padinger, F.; Fromherz, T.; Hummelen, J. C. *Appl. Phys. Lett.* **2001**, *78*, 841.
(19) Theander, M.; Yartsev, A.; Zigmantas, D.; Sundström, V.; Mammo, W.; Andersson, M. R.; Inganäs, O. *Phys. Rev. B* **2000**, *61*, 12957.
(20) Markov, D. E.; Tanase, C.; Blom, P. W. M.; Wildeman, J. *Phys. Rev. B* **2005**, *72*, 045217.
(21) Markov, D. E.; Hummelen, J. C.; Blom, P. W. M.; Sieval, A. B. *Phys. Rev. B* **2005**, *72*, 045216.
(22) Barbour, L. W.; Pensack, R. D.; Hegadorn, M.; Arzhantsev, S.; Asbury, J. B. *J. Phys. Chem. C* **2008**, *112*, 3926.
(23) Brabec, C. J.; Zerza, G.; Cerullo, G.; De Silvestri, S.; Luzzati, S.; Hummelen, J. C.; Sariciftci, S. *Chem. Phys. Lett.* **2001**, *340*, 232.
(24) Lewis, A. J.; Ruseckas, A.; Gaudin, O. P. M.; Webster, G. R.; Burn, P. L.; Samuel, I. D. W. *Org. Electron.* **2006**, *7*, 452.
(25) DeLongchamp, D. M.; Vogel, B. M.; Jung, Y.; Gurau, M. C.; Richter, C. A.; Kirillov, O. A.; Obrzut, J.; Fischer, D. A.; Sambasivan, S.; Richter, L. J.; Lin, E. K. *Chem. Mater.* **2005**, *17*, 5610.
(26) Hao, X. T.; Hosokai, T.; Mitsuo, N.; Kera, S.; Okudaira, K. K.; Mase, K.; Ueno, N. *J. Phys. Chem. B* **2007**, *111*, 10365.
(27) Boudrioua, A.; Hobson, P. A.; Matterson, B.; Samuel, I. D. W.; Barnes, W. L. *Synth. Met.* **2000**, *111*−*112*, 545.
(28) Ramsdale, N. C.; Greenham, C. M. *Adv. Mater.* **2002**, *14*, 212.
(29) Kersting, R.; Mollay, B.; Rusch, M.; Wenisch, J.; Leising, G.; Kauffmann, H. F. *J. Chem. Phys.* **1997**, *106*, 2850.
(30) Woo, H. S.; Lhost, O.; Graham, S. C.; Bradley, D. D. C.; Friend, R. H.; Quattrocchi, C.; Brédas, J. L.; Schenk, R.; Müllen, K. *Synth. Met.* **1993**, *59*, 13.
(31) Mikhnenko, O. V.; Cordella, F.; Sieval, A. B.; Hummelen, J. C.; Blom, P. W. M.; Loi, M. A. *J. Phys. Chem. B* **2008**, *112*, 11601.
(32) Ruini, A.; Caldas, M. J.; Bussi, G.; Molinari, E. *Phys. Rev. Lett.* **2002**, *88*, 206403.
(33) Nguyen, T. Q.; Schwartz, B. J.; Schaller, R. D.; Johnson, J. C.; Lee, L. F.; Haber, L. H.; Saykally, R. J. *J. Phys. Chem. B* **2001**, *105*, 5153.
(34) Tikhoplav, R. K.; Hess, B. C. *Synth. Met.* **1999**, *101*, 236.
(35) Hess, B. C.; Kanner, G. S.; Vardeny, Z. *Phys. Rev. B* **1993**, *47*, 1407.
(36) Loi, M. A.; Mura, A.; Bongiovanni, G.; Cai, Q.; Martin, C.; Chandrasekhar, H. R.; Chandrasekhar, M.; Graupner, W.; Garnier, F. *Phys. Rev. Lett.* **2001**, *86*, 732.

JP9012637